

Mathematical Corrections Applied to Laser Radar Measurements Made through a Cryogenic Vacuum Chamber Window

Joseph Hayden^a, David Kubalak^b, Theodore Hadjimichael^b, Raymond Ohl^b, Randal Telfer^c,
Bente Eegholm^a

^a Sigma Space, Lanham, 4600 Forbes Blvd, MD, 20706

^b NASA Goddard Space Flight Center, Greenbelt, MD, 20771

^c Orbital Sciences Corp., 7500 Greenway Center Dr., Beltsville, MD 20705

ABSTRACT

Laser Radar (LR) measurements were made through a vacuum chamber window for cryogenic metrology of targets attached to two different alignment fixtures used for the James Webb Space Telescope. The range and pointing errors imparted on the LR beam transmitted through up to four different optical environments resulted in reported LR distance errors of up to 22 mm, or roughly half the total single-pass glass path. These optical environments included: the air outside the chamber where the LR resides, the chamber window, the chamber environment, and the glass forming a solid glass retroreflector (SGR) target. Custom MATLAB software was developed to correct the measured laser-radar-through-the-window (LRTW) coordinates in post-processing. The software employs real ray tracing combined with a closed-form optical path length solution to resolve pointing and ranging errors caused by the phase- and group- refractive indices, respectively. The optical prescription used for ray tracing is established with knowledge of the environmental and physical parameters associated with each of the environments. The LRTW correction code shows agreement with independently developed FRED optical ray trace scripts to less than 1 μm average distance for identical environmental input parameters. The LRTW correction code was also verified by comparing LRTW corrected targets at ambient temperature and pressure on the JWST alignment fixtures to those same targets when measured with no window in place. The resulting average distance error was less than 30 μm (2-sigma), which is consistent with LR-related sources of measurement error for this test configuration. The LRTW coordinate correction software could also be used “in reverse” to calculate apparent target locations for LR measurements made through a window given the blueprint or nominal values of those targets. This capability is useful for allowing the LR to quickly locate targets measured through a window or when setting up scan boundaries around poorly illuminated distant targets. This LRTW correction capability has also recently been extended to use with Laser Trackers (LT).

Keywords: Laser radar, laser trackers, cryogenic testing, James Webb Space Telescope

1. INTRODUCTION

Two different alignment fixtures called the Master Alignment Test Fixture (MATF) and the ISIM (Integrated Science Instrument Module) Alignment Test Fixture (IATF) [1] were measured through the window of a vacuum chamber at NASA Goddard Space Flight Center (NASA/GSFC) using a Nikon Laser Radar (LR) Model MV224*. These fixtures, collectively referred to as xATF, provide a universal coordinate system reference to the Optical telescope element SIMulator (OSIM), where OSIM mimics the performance of the actual telescope optics, called the Optical Telescope Element (OTE). The LR was designed to be used at ambient temperature and pressure with a direct line of sight to the measurement target. The LR can be calibrated in air at temperatures between 5 - 40 C, pressures between 800-1100 millibar, and relative humidity ranges between 10 – 90%. The xATF targets measured lie far outside these environmental ranges with temperatures and pressures reaching as low as -238 C [35.15 K] and 10^{-5} mm Hg, respectively. Since the LR was not designed to be used directly in this extreme environment, it was necessary to mount it to the outside of the chamber to make measurements on targets inside the chamber through an

* Nikon Metrology NV, Leuven, Belgium, www.nikonmetrology.com

optical window. The targets that were measured in this cryogenic vacuum environment included 12.7 mm diameter stainless steel tooling balls, 200 μm diameter pinholes, 6.35 mm diameter through holes, and 19 mm thick solid glass retroreflectors (SGR). Although the LR was able to measure each of these targets through the uncoated chamber window without any difficulty, the reported values were incorrect since neither the LR hardware nor the commercial LR software accounted for the multiple optical media through which the LR beam was transmitted. Consequently, it was necessary to develop software to correct the LR-reported values in post-processing whereby environmental effects imparted by each of the optical media could be considered and effectively removed to give the true position of each of the targets.

2. LRTW RAY TRACE CORRECTION

Custom MATLAB code was developed at NASA/GSFC to model and correct for the refraction and range effects associated with making LR measurements through multiple optical media. Real ray tracing was used to model the refractive effects on the LR beam using known or calculated information about each of the optical media. A manually populated Excel spreadsheet was used to supply the LRTW correction software with the required optical, environmental, material, and dimensional information required to correct the apparent xyz-points measured by the LR. The LRTW correction software generated a unique optical prescription for each apparent target point to be corrected. The optical prescription, containing $i=5$ surfaces, is in the general form Z_i , R_i , n_i , and, N_i , where Z is the global position along the Z -axis at which the surface intersects the Z -axis, R is the radius of curvature, n is the phase refractive index, and N_i is the unit normal directions of the SGR entrance face.

A fixed-position LR mounted outside a vacuum chamber window was positioned with its nodal point at the origin of a coordinate system, called the *Ray Trace Frame*, whereby the Z -axis was defined to be normal to the air-side of the chamber window and the Y -axis is pointing up. The LR was roughly centered on the window so that it had a line-of-sight through the window to the targets inside the chamber. An LR beam with a wavelength of 1550 nm was transmitted through up to four different transparent optical media while measuring multiple targets inside the chamber. These optical media consisted of: 1) the ambient air around the LR outside the chamber, 2) the chamber window, and 3) the ambient or cryogenic vacuum chamber environment. It was necessary to consider a fourth optical media in the case where the target was a solid glass retroreflector (SGR) made of N-BK7. Real ray tracing was used to trace a ray from the LR nodal point through each of the optical media to the true target position, V_T . The generalized ray trace configuration is shown in Figure 1. For completeness, the SGR is shown in this ray trace diagram; however, if the target is not an SGR then the SGR thickness is set to $h=0$ so that $V_T = P_3$.

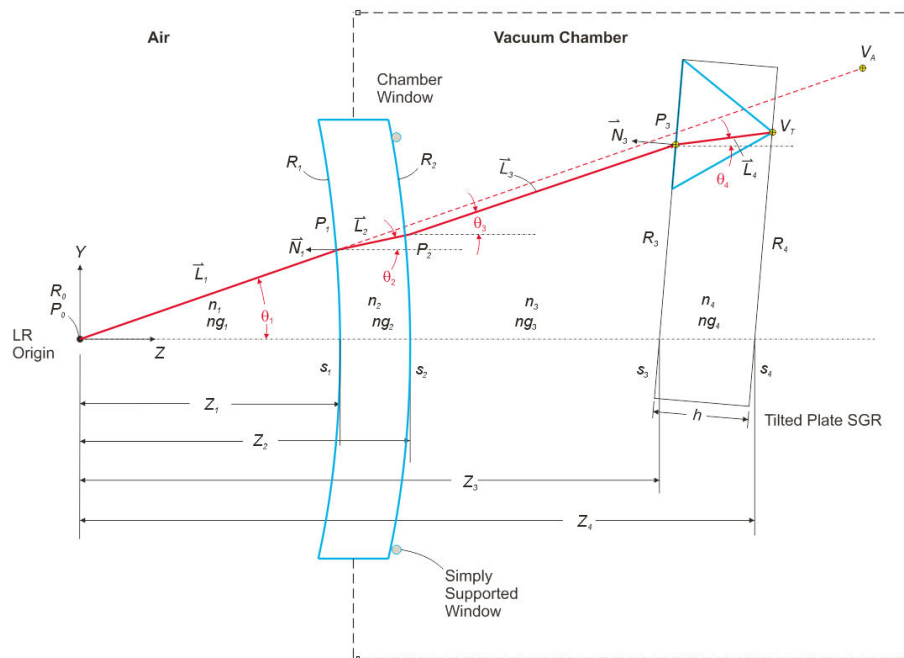


Figure 1. Test configuration to measure LR targets inside a vacuum chamber with the LR mounted outside the chamber.

The custom MATLAB[†] code uses well established vector-based refractive ray tracing methods [2], [3] to launch rays from the LR through a simple optical system. The ray trace is initiated by calculating the direction of the ray

exiting the LR nodal point as $\hat{L}_1 = \frac{\overrightarrow{P_0 V_A}}{|\overrightarrow{P_0 V_A}|}$, where the LR nodal point is $P_0 = \langle 0, 0, 0 \rangle$ and the apparent target position in the *Ray Trace Frame* is $V_A = \langle V_{Ax}, V_{Ay}, V_{Az} \rangle$. The apparent target position is the position of the target as measured and reported by the LR when the refraction and range effects associated with beam propagation through multiple optical media are not considered.

The true target position, V_T , cannot be resolved with ray tracing alone. However, by temporarily setting $Z_2 = V_{Az}$, it is possible to resolve \hat{L}_1 , \hat{L}_2 , \hat{L}_3 , and \hat{L}_4 . Note that only the direction of \hat{L}_3 is known so V_T cannot be determined until L_3 is calculated with knowledge of the corrected range.

2.1 Window Ray Tracing

The distance Z_1 between the LR, located at P0, to the first surface of the window, S1, can be determined using *direct and through*[‡] measurements, Figure 2, on a single tooling ball (TB), placed at P1, and its reflection defined by the virtual point P2. The TB position, although somewhat arbitrary, must satisfy the minimum LR to TB distance of 1 m and the LR must have lines of sight to both P1 and P2. The measurement of the virtual tooling ball at P2 requires that the signal detection parameters in the LR control software be modified to accept a low reflectance target. The low reflectivity from P2 results from the LR beam double-passing the uncoated 4% reflective window surface. The window surface, S1, is normal to the Z axis by definition of the ray trace frame.

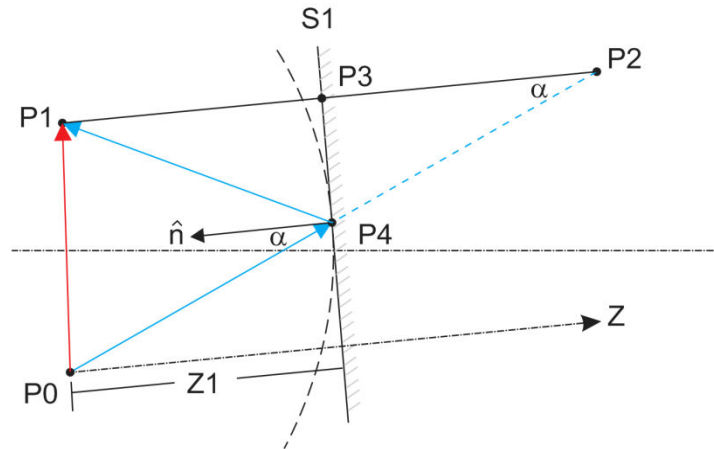


Figure 2. The *direct & through* measurements used on the first surface of the uncoated chamber window to establish the Z-axis of the Ray Trace frame, where the LR, at P0, measures a real tooling ball at P1 and the virtual TB at point P2.

The unit vector, \hat{n} , describing the normal of the first surface, S1, of the window is

$$\hat{n} = \frac{P1 - P2}{|P1 - P2|}, \quad (1)$$

where P1 and P2 are the real and virtual tooling ball (TB) points, respectively, measured by the LR.

[†] MATLAB 64-bit version 7.11.0.584 (R2010b) by MathWorks.

[‡] Spatial Analyzer Users Manual, New River Kinematics, Williamsburg, v. 1.21.2008, page 150.

The vacuum chamber window will undergo an axial deflection as a function of differential pressure that imparts a meniscus shape on the window, figure 1, where the radius of curvature, R , for either side of the window is described by Hearn [4] as

$$R = \frac{4\epsilon h^3}{3(1-\nu)(3+\nu)a^2\Delta p} \quad (2)$$

where ϵ , is the elastic modulus, h is the window thickness, ν is Poisson's Ratio, a is the radius of the simply supported window, and Δp is the pressure differential on the window. The 25.502 mm thick Fused Silica window used in our chamber resulted in a roughly 400 m radius of curvature for a differential window pressure of $\Delta p = 10^{-5}$ mm of Hg. The radius of curvature of the window is calculated, using Equation 2, for each apparent point measured by the LR based on the differential pressure on the window at the time of the measurement.

2.2 SGR ray tracing

A simple tilted plane-parallel plate model of the SGR, Figure 1, could be used by requiring that all rays entering the SGR end at the apex, or mechanical vertex, of the SGR. The justification for this constraint is evident when one considers that the SGR apex is intrinsically identified. That is, only the rays that enter the SGR entrance face and end at the SGR apex are considered in the ray trace. In the case of the LR, the SGR apex is identified using a post-processing image analysis approach. In the case of the LT, a spiral beam search method is used to lock-on to the SGR apex prior to acquiring the data point. However, when the LR to SGR distance is large, or the dihedral angle error is large, it may not be possible to use the simplified SGR model. The surface normal of the SGR entrance face was determined from separate independent measurements on the adjacent co-planer mount surface of the SGR that are assumed to be the same at ambient and cryogenic temperature. The mechanical vertex was used as the reference for the SGR, rather than the nodal point, to facilitate comparisons with direct back-side measurements of the SGR mechanical vertex from the 3-plane intersection of the facets.

A thickness versus temperature correction was also applied to the SGRs using empirical data from the European Space Agency (ESA) [5] where mirostrain was defined as a function of temperature, Figure 3, using the polynomial

$$\frac{\Delta l}{l} = 10^{-6} \sum_{i=0}^3 P_i T^i \quad (3)$$

where $P_0 = -148.53$, $P_1 = 6.7335333$, $P_2 = 0.0014505$, and $P_3 = -2.8215e-005$. Using this calculation our 19 mm thick N-BK7 SGRs change thickness by -24 μm as the temperature changes from 20 C to -238 C for an initial thickness of 19 mm at 20 C.

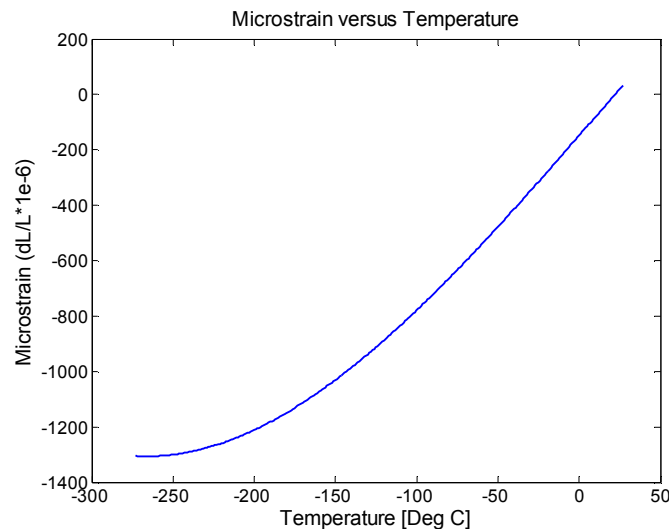


Figure 3. Plot of microstrain versus temperature for Schott N-BK7 glass determined from average of ESA data.

2.3 Absolute Phase Refractive Index

High-accuracy time-of-flight instrumentation such as the LR uses Edlen's equation [6], [7], [8], to calculate the absolute phase refractive index of air as a function of the air pressure, temperature, and relative humidity. The LR is equipped with an external environmental sensor that provides pressure, temperature, and relative humidity input to the Edlen's equation for all measurements made by the LR. However, in the case where the vacuum chamber contains air which is separated from the air outside the chamber, a separate phase refractive index must be calculated using Edlen's equation using input from the appropriate sensors placed inside the air-filled vacuum chamber. The phase refractive index is used with the real ray tracing to model refractive effects at the interfaces.

The absolute phase refractive index of the glass window and the glass SGR are described by the temperature- and wavelength-dependent modified Sellmeier dispersion equation [9], [10], using

$$n(\lambda, T) = \sqrt{1 + \sum_{i=1}^3 \frac{S_i(T) \cdot \lambda^2}{\lambda^2 - \lambda_i^2(T)}} \quad (4)$$

where

$$S_i(T) = \sum_{j=0}^4 S_{ij} \cdot T^j \quad (5)$$

And

$$\lambda_i(T) = \sum_{j=0}^4 \lambda_{ij} \cdot T^j \quad (6)$$

3. LRTW RANGE CORRECTION

Determination of the true target position, V_T in figure 1, from the LR-measured apparent target position, V_A , requires that real ray tracing be combined with a closed-form range correction equation. The range correction equation uses the results of the real ray trace, namely \bar{L}_1 , \bar{L}_2 , \bar{L}_3 , and \bar{L}_4 , combined with the calculated group refractive indices for each optical media, to solve for the true target position.

3.1 Group Refractive Index

When a pulse of light from either an LR or LT is propagated through a dispersive media the modulation envelope advances at a velocity that is different from the phase velocity of the waveform. Consequently, the group refractive index [11] must be used when modeling the range effects. Both the phase- and group-index of light propagating through a dispersive medium have a wavelength and temperature dependence. For a homogeneous dispersive media the group index, n_g , is related to the phase index, n , by

$$n_g = n + k \frac{dn}{dk} \quad (7)$$

where $k = \frac{1}{\lambda}$.

The group index for the air is calculated using a closed-form solution for dn/dk , from Edlen's equation, to model range effects. The group refractive indices for the Corning Fused Silica 7980 chamber window and the N-BK7 SGR are calculated from the derivative of the phase refractive index in Equation 4 to get

$$\frac{dn}{dk} = \frac{k}{n} \sum_{j=1}^3 \frac{S_j \lambda_j}{(1 - \lambda_j k^2)^2} \quad (8)$$

The absolute phase refractive index, n , and absolute group refractive index, n_g , Figure 4, of the Corning Fused Silica 7980 chamber window and the N-BK7 SGR are calculated using Equations (4) - (8) at the fixed LR wavelength of 1550 nm. Equations (4), (5), (6), and (8) are based on the modified Sellmeier equation and the CHARMS coefficients in Table 1 (a).

Table 1. Coefficients for the temperature-dependent Sellmeier fit of the refractive index of: a) Corning Fused Silica 7980, valid for 30 K < T < 300 K, and 0.4 μm < λ < 2.6 μm , and b) N-BK7, valid for 50 K < T < 300K, and 0.45 μm < λ < 2.7 μm .

(a) CHARMS coefficients for Corning Fused Silica 7980 glass						
Term	S_1	S_2	S_3	L_1	L_2	L_3
T^0	1.10127E+00	1.78752E-05	7.93552E-01	-8.90600E-02	2.97562E-01	9.34454E+00
T^1	-4.94251E-05	4.76391E-05	-1.27815E-03	9.08730E-06	-8.59578E-04	-7.09788E-03
T^2	5.27414E-07	-4.49019E-07	1.84595E-05	-6.53638E-08	6.59069E-06	1.01968E-04
T^3	-1.59700E-09	1.44546E-09	-9.20275E-08	7.77072E-11	-1.09482E-08	-5.07660E-07
T^4	1.75949E-12	-1.57223E-12	1.48829E-10	6.84605E-14	7.85145E-13	8.21348E-10

(b) CHARMS coefficients for N-BK7 (or BK7) glass						
Term	S_1	S_2	S_3	L_1	L_2	L_3
T^0	1.07036E+00	2.02896E-01	8.50659E-01	8.20884E-02	1.41222E-01	9.38638E+00
T^1	1.75658E-03	-1.75289E-03	1.03233E-03	4.35600E-05	-5.41379E-05	5.24515E-03
T^2	-4.28401E-06	4.18934E-06	-6.88935E-06	5.85421E-08	4.72890E-06	-3.54202E-05
T^3	-1.65687E-11	4.52824E-10	2.56510E-08	-4.13612E-10	-2.73546E-08	1.32249E-07
T^4	7.55467E-12	-8.18792E-12	-4.71564E-11	5.61059E-13	8.01380E-11	-2.38407E-10

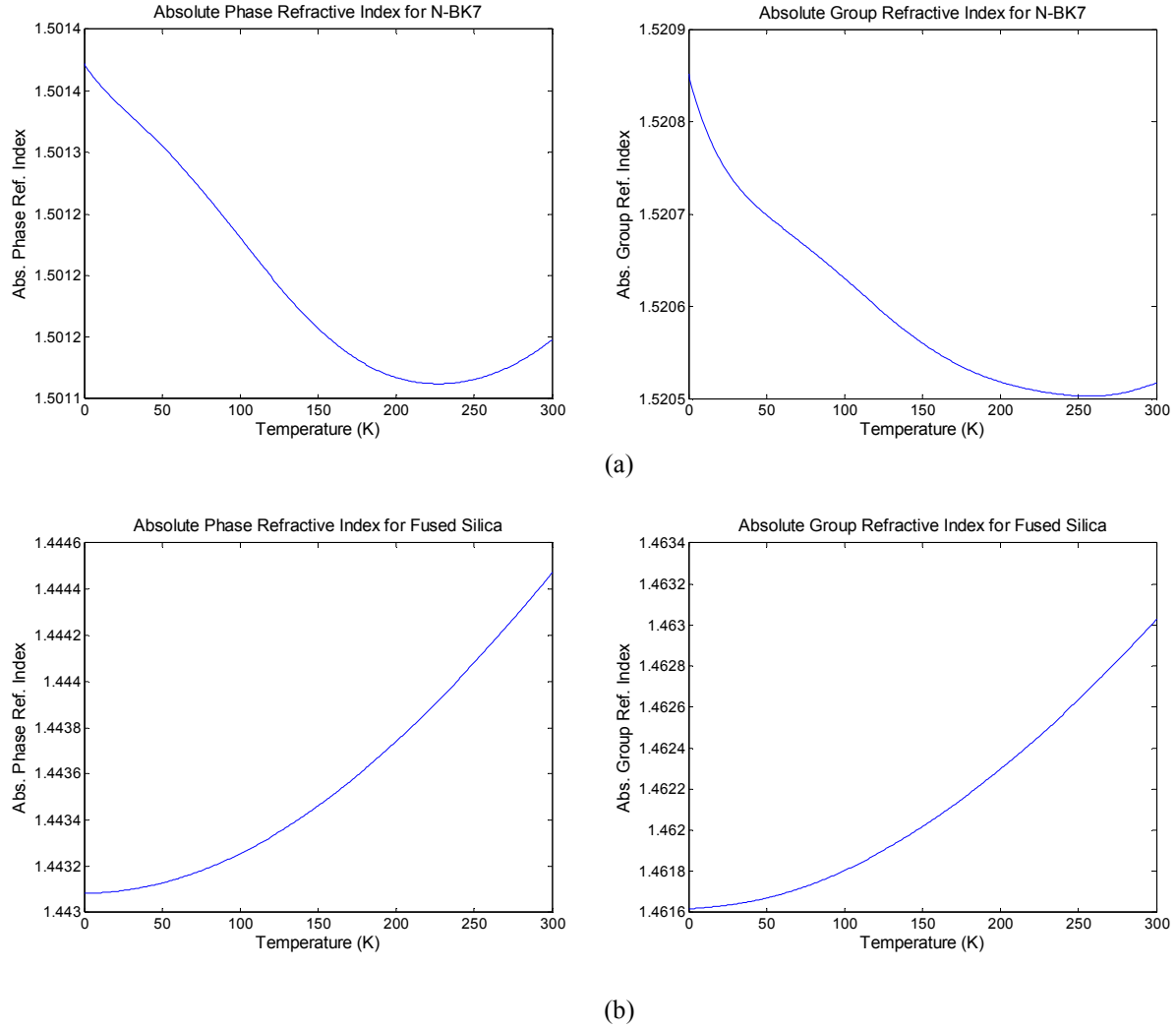


Figure 4. Plots of absolute *phase* and *group* refractive indices versus temperature for a) N-BK7, and for b) Corning Fused Silica 7980, generated using the wavelength- and temperature-dependent Sellmeier equation with corresponding CHARMS coefficients.

3.2 Range Correction Equation

The true total geometric path length of the LR beam as it travels from P_o to V_T through four optical media is

$$L_T = L_1 + L_2 + L_3 + L_4 \quad (9)$$

where L_i , for $i=1,2,3,4$, is the geometric length of the ray in each of the optical media. The optical path length measured by the LR is

$$L_A n g_1 = L_1 n g_1 + L_2 n g_2 + L_3 n g_3 + L_4 n g_4, \quad (10)$$

where L_A is the apparent total geometric length of the LR beam, and n_{g_i} , for $i=1,2,3,4$ is the group index of each of the optical media. Solving for L_3 gives the closed-form range equation

$$L_3 = \frac{(L_A n_{g_1} - L_1 n_{g_1} - L_2 n_{g_2} - L_4 n_{g_4})}{n_{g_3}}. \quad (11)$$

Finally, using this equation with the values \vec{L}_1 , \vec{L}_2 , \vec{L}_3 , and \vec{L}_4 determined from the ray trace, and using the calculated group refractive indices for each of the optical media, the true target position, \vec{V}_T , can be resolved by vector addition of the rays in each of the optical media as

$$\vec{V}_T = \vec{L}_1 + \vec{L}_2 + \vec{L}_3 + \vec{L}_4. \quad (12)$$

4. APPARENT TARGET POSITIONS FROM NOMINAL TARGET POSITIONS

Another capability of the LRTW software is to calculate apparent target positions, \vec{V}_A , given the true or nominal target positions, \vec{V}_T . This capability is useful for allowing the LR to quickly locate targets measured through a window or when setting up scan boundaries around poorly illuminated distant targets. Occasionally, it is also helpful to convert LR measurements made on metrology targets in a lab to their corresponding values in a particular vacuum chamber environment when measured through a window. The apparent target position, \vec{V}_A , can be calculated by using the LRTW code in an optimization loop to minimize $|\vec{V}_T - \vec{V}'_T|$, where \vec{V}'_T is the current calculated true target position using guess \vec{V}'_A for the apparent target position, or $\vec{V}'_T = \text{LRTW}(\vec{V}'_A)$. The optimization loop modifies \vec{V}'_A until the merit function has been satisfied. The optimization is initialized with $\vec{V}'_A = \vec{V}_T$ as \vec{V}_T is sufficiently close to \vec{V}_A to allow rapid convergence.

5. RESULTS

Targets such as pinholes, thru-holes, and SGRs used on JWST alignment fixtures were successfully measured through a window and corrected for range and pointing errors. The LRTW correction code was verified by comparing the LRTW corrected targets on the JWST alignment fixture targets with the same targets measured with no window in place. The resulting average distance error was less than 30 μm (2-sigma), which is consistent with LR-related sources of measurement error for this test configuration. The LRTW correction code showed agreement with independently developed FRED optical ray trace scripts to less than 1 μm average distance for identical environmental input parameters. The LRTW coordinate correction software could also be used “in reverse” to calculate apparent target locations for LR measurements made through a window given the blueprint or nominal values of those targets. Although this paper primarily references use of the LR for the measurement and correction of targets in a vacuum chamber, it has been demonstrated that the same equations are valid for correcting LT measurements made through a vacuum chamber window.

6. SUMMARY

It has been shown that post processing methods can be used to correct the effects of using high-performance optical metrology instruments, like the LR and LT, to make measurements on structures and targets residing in a cryogenic vacuum environment. As the need for cryogenic metrology on space hardware continues to increase there will be an increasing need to improve the efficiency of these methods. It is estimated by these authors that by incorporating LRTW correction capability into commercial metrology software the time required to determine the true position from the apparent measured position could be reduced from hours to seconds. Provided that the metrology software accepts the necessary environmental sensor inputs, the LRTW corrections could effectively be made in real-time. Also, in order to further improve the accuracy of LRTW corrections, it would be necessary to network multiple metrology devices together. This would require that optimization and bundling algorithms have knowledge of the opto-mechanical properties and uncertainties of the media through which the beams propagate.

REFERENCES

1. T. Hadjimichael, D. Kubalak, A. Slotwinski, P. Davila, B. Eegholm, W. Eichhorn, J. Hayden, E. Mentzell, R. Ohl, G. Scharfstein, and R. Telfer "Cryogenic metrology for the James Webb Space Telescope Integrated Science Instrument Module alignment target fixtures using laser radar through a chamber window", Proc. SPIE 7793, 77930B (2010).
2. Foley, J. D., and Van Dam, A. "*Computer Graphics: Principles and Practice, Second Edition*" Addison-Wesley New York, N.Y. 1990.
3. Glassner, A. (ed) "*An Introduction to Ray Tracing*" Academic Press New York, N.Y. (1989).
4. D. Hearn, "Vacuum window optical power induced by temperature gradients", SPIE Vol. 3750, July (1999)
5. S. Roose (CSL), *Evaluation of CTE measurement techniques of thermally stable materials*, Document number CSL-RP-CTEM-10001, Issue 1, 15 Dec 2010, Deliverable Item Number 6, Contract Number 21975/08/NL/SFe, European Space Agency
6. K.P. Birch and M.J. Downs, "*An updated Edlén equation for the refractive index of air*", Metrologia 30, 155-162 (1993) K.P. Birch and M.J. Downs, "An updated Edlén equation for the refractive index of air," Metrologia 30, 155-162 (1993)
7. K.P. Birch and M.J. Downs, "Correction to the updated Edlén equation for the refractive index of air", Metrologia 31, 315-316 (1994).
8. G. Bonsch and E. Potulski, "Measurement of the refractive index of air and comparison with modified Edlén's formulae", Metrologia 35, 133-139 (1998).
9. D. Leviton, B. Frey, "Temperature-dependent absolute refractive index measurements of synthetic fused silica", Proc of SPIE Vol. 6273,
10. D. Leviton, B.J. Frey, "Cryogenic, High-Accuracy, Refraction Measuring System (CHARMS) – a new facility for cryogenic infrared through far-ultraviolet refractive index measurements", SPIE, Glasgow, June, 2004.
11. E. Hecht, "*Optics, Fourth Edition*", Addison Wesley, (2002).